

Automated analysis of craniofacial morphology using magnetic resonance images

M. M. Chakravarty^{1,2}, R. Aleong¹, G. Leonard³, M. Peron⁴, G. B. Pike³, L. Richer⁵, S. Veillet⁴, Z. Pausova^{6,7}, and T. Paus^{1,7}

¹Rotman Research Institute, Baycrest, Toronto, Ontario, Canada, ²Mouse Imaging Centre, The Hospital for Sick Children, Toronto, Ontario, Canada, ³Montréal Neurological Institute, McGill University, Montréal, Québec, Canada, ⁴CÉGEP de Jonquière, Jonquière, Quebec, Canada, ⁵Département des sciences de l'éducation et de psychologie, Université du Québec à Chicoutimi, Chicoutimi, Québec, Canada, ⁶The Hospital for Sick Children, Toronto, Ontario, Canada, ⁷School of Psychology, University of Nottingham, Nottingham, United Kingdom

Introduction: Anthropologists have long used skull remains to analyze migration pattern and evolutionary-related variations of craniofacial structures in humans, Neanderthals and hominids [1,2]. Biomedical research has recently started using craniofacial phenotypes in the context of brain dysfunction (such as schizophrenia [3] and Down's syndrome [4]), hormonal environments [5], and sexual dimorphism [6]. Many of these studies have used photographs [3,4,5] and advanced laser-scanning techniques in order to generate and analyze the geometry of craniofacial structure. Given its three-dimensional nature, magnetic resonance imaging (MRI) represents an ideal imaging modality for the analysis of craniofacial structure in living individuals. The current work is motivated by the availability of MR images collected in a number of large neuroimaging initiatives, the abundance of state-of-the-art techniques for image processing of brain MR images, readily available statistical techniques for voxel-wise analyses, and the research interest in craniofacial morphology. Here, we present a voxel-based analysis and a decomposition of specific facial features using principal components analysis (PCA).

Methods: In this study we used T1-weighted data from the Saguenay Youth Study [7] to analyze the sexual dimorphism in the adolescent face (597 subjects total). Demographics are given in Table 1. In order to estimate differences in shape between faces within the population, a group-wise nonlinear average of the craniofacial features was estimated using methods similar to those used in the deformation-based analysis of brain anatomy in humans [7] and animals [8]. All linear [9] and nonlinear [10] transformations were estimated using the *mni_autoreg* package from the MINC toolbox. All MRI volumes were rigidly rotated and translated (3 rotations and 3 translations) to match an initial, randomly chosen target. The brain was then extracted, leaving only craniofacial information in each of the images. As a result of the brain extraction, the following linear and nonlinear registration steps are driven only by intensity information in craniofacial structures. All possible pair-wise 9-parameter transformations (3 rotations, 3 translations, and 3 scales) were estimated and an average linear transformation was calculated for each image, thus effectively scaling each individual scan to the average head and face size of the population. After applying the average transformation, scans were averaged and the original scans were registered to this model using a 12-parameter transformation (3 rotations, 3 translations, 3 scales, and 3 shears); a new population-based average was estimated at this point. This model represents the population atlas accounting for all linear differences in head size. A multi-generation, multi-resolution fitting strategy was then initialized where each head is nonlinearly registered to the 12-parameter population atlas, and subsequently to the atlas of the previous nonlinear registration. Table 2 contains all nonlinear transformation estimation parameters. Deformation fields were analyzed for sexual dimorphism in craniofacial structure. Craniofacial structures were also analyzed by placing landmarks on craniofacial features visible on a surface representation of the final average. These coordinate positions were warped using the nonlinear transformation and analyzed using PCA. Sexually dimorphic facial features were analyzed using the subject-wise PCA scores and simulations of each PC were performed by displacing each landmark from the average using loadings from each principal component (PC) and warping the craniofacial surface average using a thin-plate spline.

Results: The final nonlinear deformation fields maps each of the subjects' craniofacial structure to the final atlas. See Fig. 1a for the population averages obtained at each iteration of the model building process. Each deformation field was blurred with an 8-mm Gaussian kernel and the Jacobian determinant [10], a measure of local volumetric expansion and contraction, was estimated at each voxel. The voxel-by-voxel analysis [11] (correction using Gaussian Random Field Theory at $p < 0.05$) demonstrated clear sexual dimorphism (Figs 1b and 1c). The landmark-based analysis (Fig 1d) demonstrated that the first 10 principal components (PC) accounted for 80% of the variance in the data. The subject-wise scores on third, fourth, and fifth PCs (Figs 1e-g) show differences between sexes ($p < 0.001$; $F = 7.41, 8.10$, and 4.80 , respectively, with age and interactions of age and sex covaried).

Conclusions: The results demonstrate how whole-head MRI data can be used to elucidate craniofacial sexual dimorphism. Both voxel-wise analyses of the deformation fields and the PCA analysis of the deformations are sensitive to craniofacial differences between sexes. These techniques could be applied to different neuroimaging databases where whole head data are acquired. Studies such as this would allow scientists to link craniofacial phenotypes to specific pathologies.

Acknowledgments: Computations were performed on supercomputing resources provided by the SciNet HPC Consortium. SciNet is funded by: the Canada Foundation for Innovation under the auspices of Compute Canada; the Government of Ontario; Ontario Research Fund - Research Excellence; and the University of Toronto.

Figure 1. (A) Each group-wise average created after LSQ9, LSQ12, and all nonlinear stages of the model building process. (B) and (C) Voxel-wise analysis of deformation fields demonstrating local volume changes specific to males and females respectively. (D) Craniofacial landmarks on surface model of population average. (E), (F), and (G) Simulations of 0.6 of the loadings for PCs 3-5.

Table 1 Demographics for all participants.

| | Males | Females |
|------------------------------|--------------|--------------|
| Participants | 292 | 305 |
| Mean Age in Months (Std Dev) | 180.5 (22.2) | 181.8 (23.0) |
| Full-scale IQ (Std Dev) | 104.3 (14.6) | 104.2 (13.2) |

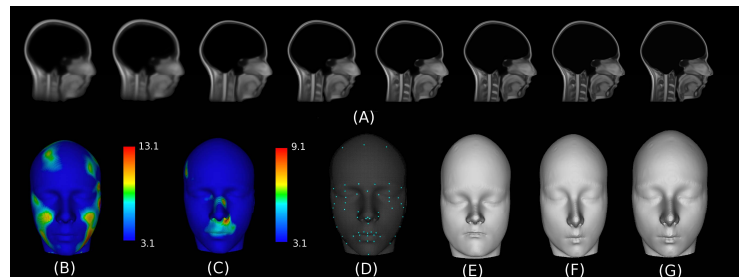


Table 2 Nonlinear registration parameters

| Step size (mm) | Iterations | Gaussian Blur (mm) |
|----------------|------------|--------------------|
| 8 | 30 | 16 |
| 8 | 30 | 8 |
| 4 | 30 | 8 |
| 4 | 30 | 4 |
| 2 | 10 | 4 |
| 2 | 10 | 2 |

References

- [1] P. Mitteroecker *et al.* Evolution and Development 7:244-258.
- [2] Harvati *et al.* Journal of Human Evolution 59: 445-64.
- [3] Kelly *et al.* Schizophrenia Research 80:349-44.
- [4] Cohen *et al.* Journal of Craniofacial Surgery 6:184-9.
- [5] Fink *et al.* Proceedings of the Royal Biological Society 272: 1995-2001.
- [6] Hennessy *et al.* Biological Psychiatry 51:507-14.
- [7] Pausova *et al.* Human Brain Mapping 28:502-518.
- [8] Borghammer *et al.* European Journal of Neurology 17:3145-20.
- [9] Lerch *et al.* NeuroImage 39:32-9.
- [10] Collins *et al.* Journal of Computer Assisted Tomography 18:192-205.
- [11] Collins *et al.* Human Brain Mapping 3:190-208.
- [12] Chung *et al.* NeuroImage 4:595-15.
- [13] Worsley *et al.* NeuroImage 15:1-15.